Structure and Phase Behavior of Mixed Monolayers of Saturated and Unsaturated Fatty Acids

Benjamin M. Ocko* and Michael S. Kelley[†]

Department of Physics, Brookhaven National Laboratory, Upton, New York 11973

Ani T. Nikova[‡] and Daniel K. Schwartz[§]

Department of Chemistry, Tulane University, New Orleans, Louisiana 70118

Received June 17, 2002. In Final Form: October 2, 2002

Grazing incidence X-ray diffraction (GIXD) and Brewster angle microscopy (BAM) were used to study the miscibility and phase behavior of Langmuir monolayers composed of a mixture of a saturated (stearic) and a trans-monounsaturated (elaidic) fatty acid. In contrast with suggestions from previous thermodynamic measurements, these compounds were poorly miscible in monolayers, and phase separation was always observed between domains of a liquid crystalline stearic acid-rich phase and a disordered elaidic acid-rich phase. The molecular packing density inside the ordered domains of mixed monolayers was within 2% of the density of pure stearic acid monolayers at the same surface pressure, suggesting that this phase contained at most a very small fraction of the larger elaidic acid molecules. However, the presence of this small concentration of unsaturated chains depressed the L_2 to Ov phase transition by ∼7 mN/m.

1. Introduction

A comprehensive understanding of the structure and phase behavior of saturated fatty acid Langmuir monolayers[1] has emerged over the past 15 years. This development has been spurred by the advent of synchrotron radiation, surface X-ray scattering techniques, and Brewster angle microscopy. A universal phase diagram (temperature and pressure) has been determined for saturated fatty acids in which seven different ordered phases form, characterized by differences in the tilt direction and the lateral distortions from a hexagonal lattice.[1] The effects of chain length,[2,3] mixtures,[4] and pH[5] have also been investigated. Phospholipids, which are composed of a phosphatidyl headgroup linked to two fatty acids, comprise the majority of the amphiphilic molecules within biological membranes. The precise composition of the phospholipids in a given membrane (i.e., chain length, saturated vs unsaturated chains, headgroup identity, etc.) depends on the species and environmental conditions. For cell membranes to remain fluid they must contain a mixture of saturated and unsaturated fatty acids. Cell membranes in many fish, for example, contain sizable amounts of omega-3 oils (highly unsaturated), and a higher degree of omega-3 oils are found in fish in the coldest climates. In recent years, particular interest has grown in submicron domains within membranes,[6,7] known as "rafts", that are potentially important in cell signaling, are sources of proteins related to amyloid diseases, and are targets for certain pathogens. Rafts are believed to have distinctive lipid compositions; in particular, they are rich in sphingolipids with saturated chains. It has been proposed that the formation of rafts is due to the differential miscibility of various lipids within bilayer membranes.[8]

One of the most common unsaturated fatty acids found in living cells is oleic acid (OA, *cis*-9-octadecanoic acid), a monounsaturated fatty acid. It is nearly identical to stearic acid (SA, *n*-octadecanoic acid) except that it contains a cis double bond in the middle of the chain. This gives rise to a bent shape of OA relative to SA, a linear molecule. This bent shape also hinders crystallization and explains why the bulk melting temperature of OA (13 °C) is considerably lower than that of SA (72 °C). Elaidic acid (EA, *trans*-9-octadenoic acid) is the trans isomer of OA. Since EA is not as bent as OA, it can pack more efficiently and has a higher melting point (44 °C).

Langmuir monolayers of EA and OA along with mixtures were first investigated by Harkins and Florence[9] and more recently by Feher, Collins, and Healy.[10] Despite their very different bulk melting temperatures, EA and OA have similar pressure−area isotherms.[10] For both EA and OA, the surface pressure starts to increase from zero at about 55−60 Å^2 per molecule, which is more than twice the area where the surface pressure of SA begins to increase. The 55−60 Å^2 per molecule is slightly less than half the area of a lying down molecule and nearly 3 times the cross-sectional area of a saturated *n*-alkane. These large areas as well as the shape of the isotherms for the monounsaturated fatty acids (concave upward instead of linear) are generally interpreted as evidence that the monolayers are in a 2D liquid state as opposed to a condensed liquid crystalline or solid phase. In contrast, the small limiting area and linear shape of the SA isotherm

[†] Current address: School of Physics and Astrophysics, University of Minnesota, Minneapolis, MN 55455.

[‡] Current address: Division of Engineering and Applied Science, Harvard University, Cambridge, MA 02138.

[§] Current address: Department of Chemical Engineering, University of Colorado, Boulder, CO 80309-0424.

(1) Kaganer, V.; Mohwald, H.; Dutta, P. *Rev. Mod. Phys.* **1999**, *71*, 779.
(2) Bibo, A. M.; Peterson, I. R. *Adv. Mater.* **1990**, *2*, 309.
(3) Petrov, J. G.; Pfohl, T.; Mohwald, H. **1999**.
(4) Bibo, A. M.; Knobler, C.; Peterson, I. R. *J. Phys. Chem.* **1991**, *95*, 5591.
(5) Johann, R.; Vollhardt, D.; Möhwald, H. *Langmuir* **2001**, *17*, 4569.
(6) Brown, D. A.; London, E. *J. Biol. Chem.* **2000**, *275*, 17221.
(7) Brown, D. A.; London, E. *J. Membr. Biol.* **1998**, *164*, 103.
(8) Rietveld, A.; Simons, K. *Biochim. Biophys. Acta* **1998**, *1376*, 467.
(9) Harkins, W. D.; Florence, R. T. *J. Chem. Phys.* **1938**, *6*, 856.
(10) Feher, A. I.; Collins, F. D.; Healy, T. W. *Aust. J. Chem.* **1977**, *30*, 511.

10.1021/la026079y CCC: $22.00
Published on Web 11/08/2002

are consistent with a condensed phase; this has been confirmed by X-ray diffraction.[11−13]

The excess free energy of mixing, ΔG_{mix}, was calculated by Feher and co-workers for mixed monolayers of EA or OA with saturated acids, either SA or arachidic acid.[10] The positive values of ΔG_{mix} for the mixed monolayers with OA indicated an immiscible mixture, and the negative values of ΔG_{mix} with EA indicated miscibility. This was intuitively attractive given the greater similarity of molecular shape between the trans acid EA and SA. We were motivated by these results to carry out both X-ray grazing incident angle diffraction (GIXD) and Brewster angle microscopy (BAM) studies of mixed EA and SA monolayers. The former probes the local molecular packing whereas the latter addresses the existence of macroscopic immiscible regions. Our results show that EA and SA are effectively immiscible at low surface pressures, and the miscibility increases only slightly at high surface pressures. However, the presence of this small amount of EA significantly depresses the transition pressure for the L_2 to Ov transition.

2. Experimental Details

Langmuir monolayers of the EA/SA (>99%, Sigma) acid solutions were spread from either chloroform or *n*-hexane on a pH = 2 adjusted aqueous solution (Millipore Milli-Q water and nitric acid) contained in a custom-built Langmuir trough. Pure EA and SA were investigated along with SA:EA mixtures with molar ratios 70:30 and 32:68. All measurements were carried out at a temperature of 22 °C. The surface pressure was monitored by a filter paper Wilhelmy plate and an electrobalance. X-ray data were acquired in both fixed area and fixed pressure modes.

The X-ray measurements were carried out on the Harvard/BNL liquid surface spectrometer at the National Synchrotron Light Source, beam line X22B with a wavelength $\lambda = 1.54$ Å. The details of this spectrometer were described elsewhere.[14] X-ray grazing incidence diffraction experiments were performed to probe the in-plane structure of the Langmuir monolayer. Here, the incident angle, $\theta = 0.12°$, was set to be less than the critical angle for total reflection of water, $\theta_c = 0.151°$. By scanning the detector angle 2θ out of the specular plane, the scattered intensity was measured as a function of the in-plane component q_{xy}. The use of Soller slits in the detector plane (100 mm high) yielded an in-plane resolution of $\Delta q_{xy} = 0.012$ Å^{-1} fwhm. A linear detector (10 mm wide and 100 mm high) allowed us to measure the scattering along q_z over a range of 0.8 Å^{-1}. The resolution along q_z was coarsened to 0.05 Å^{-1} in order to reduce the counting noise.

Using a separate trough, the monolayer was visualized by means of a custom-built Brewster angle microscope.[15,16] Light from a 30 mW 670 nm diode laser was p-polarized and directed onto the water surface at the Brewster angle for the water subphase. The reflected light was focused onto a CCD camera by a 4× microscope objective.[17] BAM is sensitive to the properties of the interfacial film. Coexisting phases with different densities can be distinguished in the BAM images because of their different reflectivity.[15,18] By adding an analyzing polarizer to the path of the reflected beam, variation in the direction of the azimuthal tilt provides additional contrast.[19,20]

(11) Kjaer, K. J.; Als-Nielsen, J.; Helm, C. A.; Tippmann-Krayer, P.; Mohwald, H. *Phys. Rev. Lett.* **1987**, *58*, 2224.
(12) Dutta, P.; Peng, J. B.; Lin, B.; Ketterson, J. B.; Prakash, M.; Georgopoulos, P.; Ehrlich, S. *Phys. Rev. Lett.* **1987**, *58*, 2228.
(13) Peterson, I. R.; Brezesinski, G.; Struth, B.; Scalas, E. *J. Phys. Chem. B* **1998**, *102*, 9437.
(14) Ocko, B. M.; Wu, X. Z.; Sirota, E. B.; Sinha, S. K.; Gang, O.; Deutsch, M. *Phys. Rev. E* **1997**, *55*, 3164.
(15) Hénon, S.; Meunier, J. *Rev. Sci. Instrum.* **1991**, *62*, 963.
(16) Hönig, D.; Möbius, D. *J. Phys. Chem.* **1991**, *95*, 4590.
(17) Kurnaz, M. L.; Schwartz, D. K. *Phys. Rev. E* **1997**, *56*, 3378.
(18) Hénon, S.; Meunier, J. *J. Phys. Chem.* **1993**, *98*, 9148.
(19) Overbeck, G. A.; Möbius, D. *J. Phys. Chem.* **1993**, *97*, 7999.
(20) Riviére, S.; Hénon, S.; Meunier, J.; Schwartz, D. K.; Tsao, M.-W.; Knobler, C. M. *J. Chem. Phys.* **1994**, *101*, 10045.

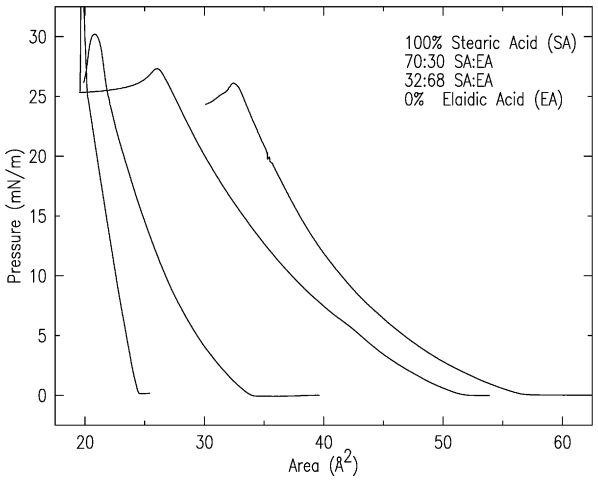

Figure 1. Isotherms for pure stearic (left curve) and elaidic (right curve) acids and for the 70:30 and 32:68 mixtures (middle curves). The data were obtained in the same trough used in the X-ray measurements.

3. Results

Isotherms. Isotherms for pure SA and EA along with two mixtures are shown in Figure 1 at 22 °C (pH = 2) for compression rates in the range of 0.5−1.0 Å^2 mol^{-1} min^{-1}. No significant differences between isotherms carried out on pure water and at pH = 2 were observed. For pure SA (pH = 2), the surface pressure increased linearly from zero starting at an area of about 25 Å^2/mol. At about 20 Å^2/mol, where the surface pressure reaches 26 mN/m, the pressure starts to increase with a much steeper slope; this corresponds to a transition from the Ov tilted phase to the untilted LS phase. At slightly smaller areas the monolayer collapses. Prior to the collapse, the isotherm was reversible within an area of about ±0.2 Å^2/mol. For pure EA, the surface pressure started to increase when the area decreases to ∼57 Å^2/mol, and a pressure of 20 mN/m was reached at an area of about 36 Å^2/mol. Whereas the slope of the isotherm was constant for SA, the surface pressure slope increased with decreasing surface area for pure EA (i.e., the isotherm is concave upward). The two mixtures of EA and SA exhibited behavior intermediate between that of their pure components. For the 70:30 and 32:68 SA:EA acid mixtures the pressure started to increase from zero at respective areas of 34 and 52 Å^2 /mol. If the two phases were completely phase separated, one would expect areas of 35 and 47 Å^2 /mol, respectively. The close agreement for the mixture rich in SA is consistent with phase-separated regions of nearly pure components. On the other hand, the discrepancy for the mixture rich in EA suggests significant mixing.

Although the isotherms containing EA were reversible at low surface areas, hysteresis effects appeared at surface pressures >10 mN/m. Further, at fixed areas the surface pressure decreased with time, and the rate of decrease increased with decreasing area. The hysteresis and loss of surface pressure can be attributed to the increased solubility of EA in the aqueous subphase compared to SA (or faster kinetics of collapse).

GIXD. Figure 2 shows the results of the GIXD measurements as equal intensity contours for pure SA and the 70:30 SA:EA acid mixture at four different surface pressures of 4 (Figure 2a,e), 8 (Figure 2b,f), 12 (Figure 2c,g), and 16 mN/m (Figure 2d,h). These resolution-limited in-plane peaks with broad features along q_z resulted from liquid-crystalline monolayer regions. For the 32:68 SA:EA mixture, very weak diffraction peaks were observed

Table 1. Summary of the X-ray Results for Pure Stearic Acid and the 70:30 Mixture of Stearic:Elaidic Acids[a]

	SA (mol %)	π (mN/m)	A_{isotherm} (Å^2)	$A_{\text{X-ray}}$ (Å^2)	q_{dxy} (Å^{-1})	q_{dz} (Å^{-1})	q_{nxy} (Å^{-1})	q_{nz} (Å^{-1})	a (Å)	b (Å)	χ (deg)	distortion
a	100	4	23.5	22.8	1.385	0.63	1.475	0.00	5.36	8.52	25.8	0.084
b	100	8	23.0	22.3	1.410	0.60	1.475	0.00	5.23	8.52	24.8	0.060
d	100	12	22.5	21.8	1.430	0.52	1.480	0.00	5.13	8.49	21.9	0.046
d	100	16	21.5	21.3	1.455	0.42	1.485	0.00	5.02	8.46	18.0	0.027
e	70	4	30.0	22.9	1.385	0.63	1.470	0.00	5.35	8.55	25.9	0.079
f	70	8	28.0	22.4	1.405	0.57	1.470	0.00	5.25	8.55	23.8	0.060
g	70	12	26.0	22.0	1.460	0.32	1.400	0.56	4.90	8.98	22.2	0.056
h	70	16	24.5	21.5	1.470	0.24	1.430	0.50	4.89	8.79	18.6	0.041

[a] The letters refer to the curves shown in Figure 2. A_{isotherm} corresponds to the area per molecule obtained from the trough area and the number of deposited molecules. The tilt and distortions were calculated according to the formulas provided in the text.

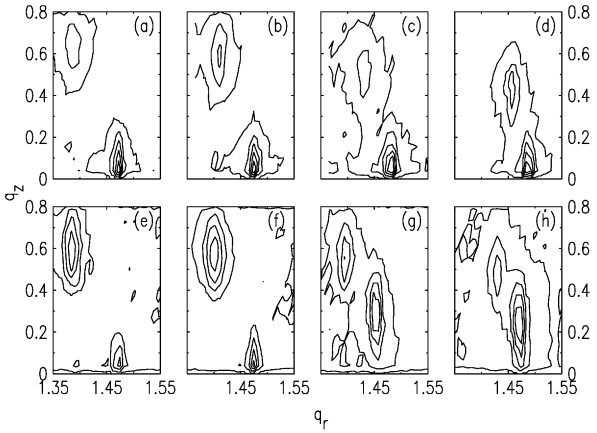

Figure 2. Equal intensity X-ray scattering contours for pure stearic acid (a−d) and for a mixture which is 70:30 SA:EA acid (e−h) at a pH = 2. These contours correspond to surface pressures of 4 (a, e), 8 (b, f), 12 (c, g), and 16 mN/m (d, h).

(not shown) at the highest pressures, but only after waiting for several hours at these pressures. The peaks in the diffraction pattern are due to the liquid-crystalline order within the surface plane. At sufficiently high surface pressures in pure SA (not shown) a single on-axis in-plane peak was observed. For pure EA (not shown) no diffraction features were observed between $1.0 < q_{xy} < 1.7$ Å^{-1} at pressures below 20 mN/m, implying that these monolayers do not form ordered phases.

Below surface pressure of about 10 mN/m, the diffraction patterns from the pure SA and the 70:30 SA:EA mixture appeared the same, exhibiting one on-axis peak and the other off-axis. In the case of the mixture, the scattering intensity was noticeably reduced. Above a surface pressure of about 10 mN/m the diffraction patterns for the two compounds were no longer the same. Whereas the pure SA diffraction pattern continued to exhibit both an on-axis and off-axis peak (Figure 2c,d), the 70:30 SA:EA mixture exhibited two off-axis peaks (Figure 2g,h), one at twice the q_z value of the other.

The two diffraction patterns observed in our measurement correspond to distorted hexagonal unit cells (centered rectangular) where the molecules are tilted from the normal axis by an angle χ. For the case where one peak is on-axis, the molecular tilt was along the nearest-neighbor (NN) direction, and this pattern corresponds to the L_2 phase. On the other hand, when both peaks were off-axis, the molecular tilt was along the next-nearest-neighbor (NNN) direction. Two phases have been observed with this symmetry, known as L_2' and Ov; the lattice parameters of the observed phase are consistent with the Ov phase.[13,21] Although both phases are distorted from hexagonal packing within the surface plane, the Ov phase is locally hexagonal within the plane defined by the long axis of the molecules

It is common to index the diffraction peaks as to whether the peaks are degenerate (q_{dxy}, q_{dz}) or non-degenerate (q_{nxy}, q_{nz}).[1,22] For the centered rectangular unit cell, the (02) reflection corresponds to the nondegenerate peak position, and the (11) and (1$\bar{1}$) positions correspond to the degenerate peaks. The rectangular unit cell dimensions (a, b) are given in Table 1.

The molecular tilt and dimensionless distortions can be calculated from the diffraction pattern according to the definitions of Kaganer.[22] According to these definitions, the distortion is given by

$$\delta = {}^8/_3(q_{nxy} - q_{dxy})/(q_{nxy} + q_{dxy})$$

The molecular tilts from the normal are given by

$$\chi = \tan^{-1}\left(q_{dz}\Big/\sqrt{q_{dxy}^2 - \left(\frac{q_{nxy}^2}{2}\right)^2}\right) \quad \text{(Ov phase)}$$

and

$$\chi = \tan^{-1}(q_{nz}/q_{nxy}) \quad (L_2 \text{ phase})$$

With increasing surface pressure both the tilt and distortion decreased, as supported by the values given in Table 1. At sufficiently high surface pressure both the tilt and distortion went to zero where the hexagonal phase forms.

For pure SA monolayers, the molecular area, calculated from diffraction data ($A_{\text{X-ray}}$), decreased continuously from 22.8 to 21.3 Å but was always within 1−3% of the molecular area based on the trough area and number of deposited molecules (A_{isotherm}). This discrepancy is typical and due to uncertainties involved with solution concentration and deposited volume. However, for the 70:30 mixture, the area A_{isotherm} was larger than $A_{\text{X-ray}}$ by amounts ranging from 14 to 30%, but $A_{\text{X-ray}}$ was always very close to the value for the pure SA monolayer at the same surface pressure. Together this suggests that the mixed monolayer had phase-separated into regions of SA and EA where the SA regions gave rise to the observed diffraction.

For the 70:30 SA:EA mixture and the pure monolayers the identical diffraction patterns below 10 mN/m corresponded to the L_2 phase; above this pressure the 70:30 SA:EA mixture exhibited the diffraction pattern from the Ov phase[21] whereas the pure monolayer continued to exhibit the L_2 phase, albeit with nearly the same molecular area and tilt as the pure SA monolayer at the same pressure (see Table 1). In the case of the mixture, the scattering intensity was noticeably reduced. For both the pure and mixed monolayers, the tilt angle decreased continuously from about 26° at 4 mN/m to about 18° at

(21) Durbin, M. K.; Malik, A.; Ghaskadvi, R.; Shih, M. C.; Zschak, P.; Dutta, P. *J. Phys. Chem.* **1994**, *98*, 1753.

(22) Kaganer, V. M.; Peterson, I. R.; Kenn, R. M.; Shih, M. C.; Durbin, M.; Dutta, P. *J. Chem. Phys.* **1995**, *102*, 9412.

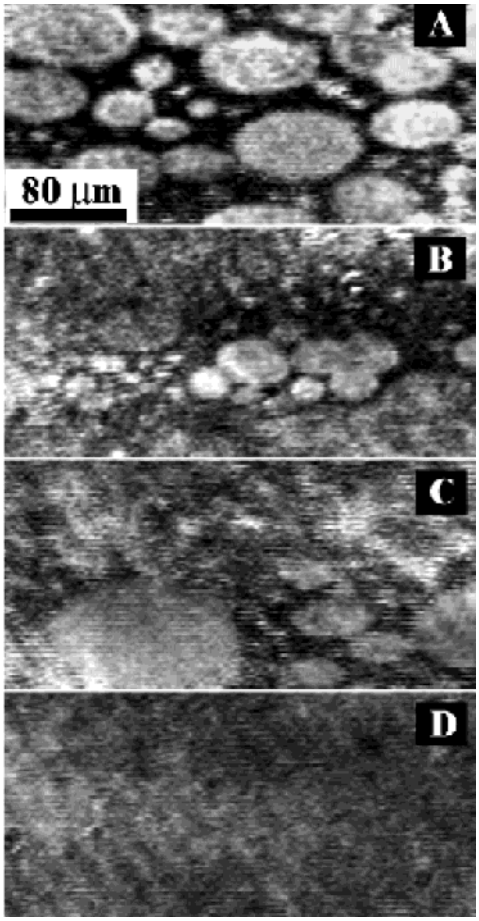

Figure 3. BAM images of a 70:30 SA:EA acid monolayer imaged without an analyzer at different surface pressures: (A) $\pi = 0.8$ mN/m, (B) $\pi = 6$ mN/m, (C) $\pi = 11.8$ mN/m, and (D) $\pi = 23$ mN/m.

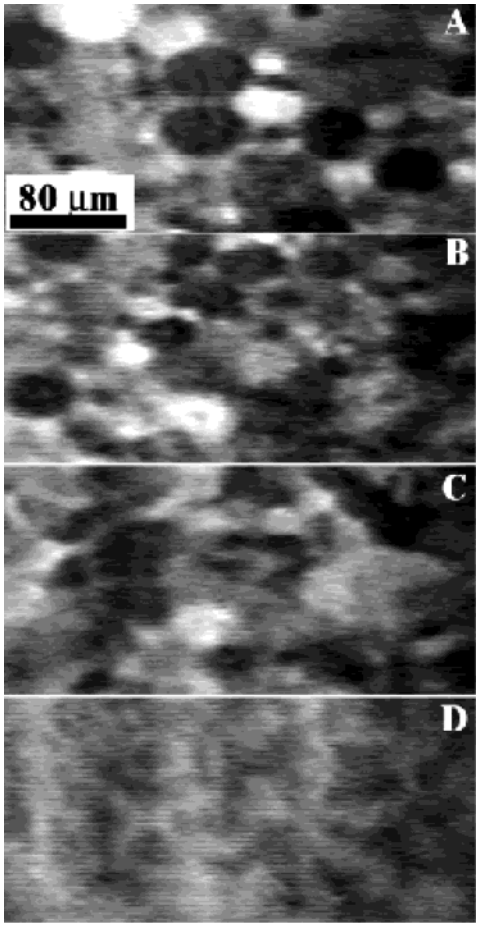

Figure 4. BAM images of a 70:30 SA:EA acid monolayer imaged with an analyzer at different surface pressures: (A) $\pi = 0.7$ mN/m, (B) $\pi = 5.8$ mN/m, (C) $\pi = 12$ mN/m, and (D) $\pi = 24$ mN/m.

16 mN/m. Finally, we note that the area per molecule, within the plane defined by the long axis of the molecules, did not exhibit a systematic variation with surface pressure or the addition of EA and is equal to 20.4 ± 0.2 Å.

BAM. Pure EA monolayers appeared uniformly gray, with or without an analyzer, suggesting a uniform disordered 2D liquid phase. BAM images of SA and other saturated fatty acids have been published previously;[19,20] the current observations were consistent with the published ones. Without an analyzer, SA monolayers appeared uniformly gray; with an analyzer the mosaic of tilt domains of differing gray values was observed. At $\pi \sim 25$ mN/m the contrast of the mosaic disappears, consistent with the loss of molecular tilt. Neither pure EA nor pure SA monolayers showed any sign of phase coexistence at nonzero surface pressures.

For the 70:30 SA:EA mixture, at low surface pressures (less than 1 mN/m), we observed a dark continuous phase that contains bright circular domains (Figure 3A) when the images were obtained without an analyzer. The circular domain shapes appear elliptical in the BAM images since the microscope is focused on the interface at the Brewster angle for water (~53° with respect to the surface normal). We note that this corresponds to a factor of ~0.6 in the vertical scale. The different reflectivity between the dark regions and the bright domains is due to differences in the molecular surface densities (in particular, the contrast is related to the difference in optical thickness) of the two regions, indicative of phase coexistence. Since the domains appear bright, they represent the more condensed phase; therefore, we cannot identify them with a "gas" phase within a mixed monolayer. We, therefore, believe that these domains are formed by a SA-rich phase, while the dark phase represents an EA-rich phase. Figure 3B−D shows a series of BAM images of the same mixed monolayer at various increasing surface pressures. As the surface pressure was increased above 5 mN/m, we observed gradual domain distortion or coalescence, accompanied by a decrease of contrast in the image. At a surface pressure close to 24 mN/m, the monolayer appeared uniform. This loss of BAM contrast at high surface pressure is typical for fatty acids and is consistent with the molecular tilt angle going to zero (i.e., normal to the interface). For $\pi > 25$ mN/m, therefore, we cannot make conclusions about phase separation on the basis of BAM images alone.

Complementary images were also obtained with an analyzer which permits observation of contrast due to molecular orientational order. As with the images obtained in the absence of the analyzer, we observed circular domains (Figure 4A). In contrast to the studies without an analyzer which exhibited a uniform level of brightness, these images show a large variation in the reflected intensity within and between domains. The combined results indicate that the domains with different intensities represent the same phase; however, they differ in the azimuthal direction of the molecular tilt with respect to the incident light beam. The presence of orientational order of the molecules within the different domains indicates that the SA-rich phase is liquid-crystalline while the uniform appearance of the surrounding regions again

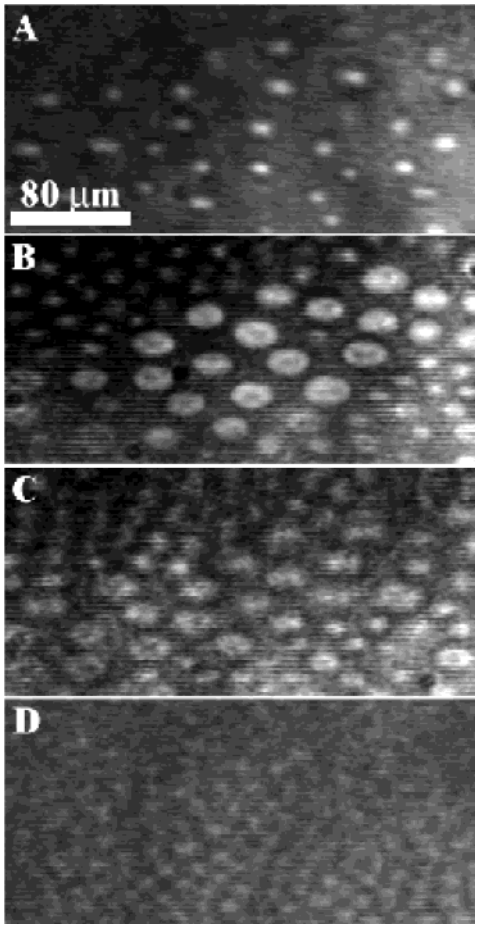

Figure 5. BAM images of a 32:68 SA:EA acid monolayer obtained without an analyzer at different surface pressures: (A) $\pi = 0.9$ mN/m, (B) $\pi = 11.9$ mN/m, (C) $\pi = 15.8$ mN/m, and (D) $\pi = 25.2$ mN/m.

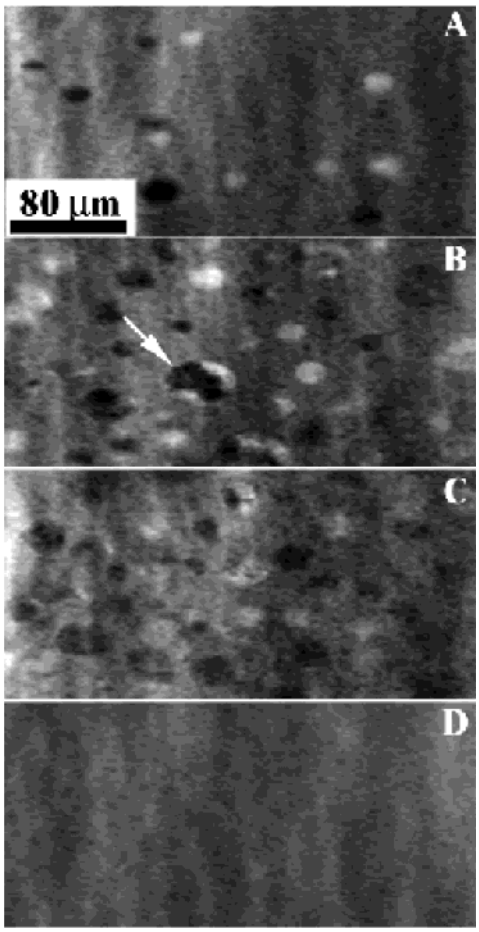

Figure 6. BAM images of a 32:68 SA:EA acid monolayer obtained with an analyzer at different surface pressures. The arrow indicates a domain that contains subdomains with different molecular tilt azimuths, resulting in different reflectivity. (A) $\pi = 0.5$ mN/m, (B) $\pi = 12$ mN/m, (C) $\pi = 16$ mN/m, and (D) $\pi = 25$ mN/m.

suggests that the EA-rich phase is a disordered liquid. As the monolayer is compressed to $\pi \sim 5$ mN/m, domains appeared to distort from their circular shape (Figure 4B). Upon further increase of surface pressure the domain structure started to disappear, as seen in Figure 4C, and the overall contrast of the image decreased. At $\pi \sim 24$ mN/m (Figure 4D) the monolayer appeared as a uniform film. This was close to the surface pressure where a pure SA monolayer undergoes a transition to an untilted phase.[23]

We have also carried out microcopy studies of a 32:68 SA:EA mixture. As for the SA-rich mixture, we observed bright circular domains within a dark phase at surface pressures below 1 mN/m (Figure 5A). The typical domain size within the continuous phase was smaller than those observed in the 70:30 SA:EA monolayer at the same surface pressure. Furthermore, the area fraction of the domains was smaller. This observation is again consistent with the interpretation that the domains represent an SA-rich phase; the domains are smaller in this case because the SA volume fraction is reduced. Compression of the monolayer to $\pi \sim 12$ mN/m resulted in growth of larger domains (Figure 5B). With further increase of the surface pressure, the contrast in the image decreased (Figure 5B) and eventually disappeared at ~25 mN/m (Figure 5D). Images acquired with an analyzer (Figure 6A) again displayed a large variation in the reflected signal from domain to domain. We also observed regions where the reflectivity varies within a single domain (indicated by the arrow in Figure 6B). This is additional evidence that the molecules within the domains possess liquid-crystalline order. Compression to higher surface pressure resulted in distortion of the domain structure and a decreased image contrast (Figure 6C) until a uniform film was formed at $\pi \sim 25$ mN/m, as seen in Figure 6D.

4. Discussion

The BAM images constitute clear evidence that EA and SA are far from completely miscible. In fact, they separate, even at low surface pressure, into domains of a liquid-crystalline phase dispersed within a disordered liquid phase. X-ray data obtained at low surface pressure demonstrate that the molecular density within the ordered phase is identical to that of a pure SA monolayer at the same surface pressure (within experimental uncertainty), and the details of packing correspond to the L_2 phase. This suggests that the solubility of EA within the ordered SA-rich domains must be very small; a large concentration of EA would likely result in significant expansion of the molecular lattice.

At ~10 mN/m, in the 70:30 SA:EA mixture, the results suggest a transition from the L_2 to the Ov phase within the condensed phase domains. This occurs at a significantly reduced surface pressure in the mixture than in a pure SA monolayer (~18 mN/m at 22 °C). These observations suggest that the presence of EA has a significant

(23) Schwartz, D. K.; Knobler, C. M. *J. Phys. Chem.* **1993**, *97*, 8849.

effect on the phase transition and on the structure of the high-pressure Ov phase, in contrast with the negligible effect on the low-pressure L_2 phase. The molecular area within the ordered domains is slightly expanded (<2%) relative to that of molecules in pure SA at the same pressure. This could be due to increased solubility of EA in this phase; however, it may simply be a function of fundamental differences in the packing efficiency of the two phases so conclusions regarding increased miscibility cannot be made with great confidence. It was previously shown that the addition of a long-chain alcohol[24,25] or ester[26] lowered the pressure of the L_2 to Ov transition of a saturated fatty acid monolayer. In these cases, the lowering effect was generally ascribed to headgroup effects (e.g., extent of hydrogen bonding with the subphase).[26] Clearly, in the present case the headgroups of all components are identical, and another mechanism must be at work.

The origin of the L_2 to Ov phase transition remains controversial. This transition, sometimes referred to as a swiveling transition, corresponds to the rotation of the tilt direction by 30° (plus multiples of 60°) relative to the crystallographic axis. In a recent study of the pH dependence of the phase behavior in arachidic acid, it was found that the surface pressure at the L_2 to Ov phase transition varied significantly with pH at values between 8 and 10.[5] This suggests that the headgroup bonding interactions play an important role in determining the direction of the tilt. An alternative explanation is that the transition is driven by energy differences at the domain boundaries in the absence of chain rotation.[5] Within the context of this model, the direction of the tilt with respect to the morphological features remains constant across the transition; however, the direction of the distortion changes. For the mixed SA and EA monolayers investigated in the present study, the L_2 to Ov transition might be affected by the elaidic acid which influences the line tension at the domain boundaries between the phase-separated regions.

(24) Lee, S.; Shih, M. C.; Durbin, M. K.; Malik, A.; Zschak, P.; Dutta, P. *J. Chem. Phys.* **1994**, *101*, 9132.
(25) Pischer, B.; Teer, E.; Knobler, C. M. *J. Chem. Phys.* **1995**, *103*, 2365.
(26) Teer, E.; Knobler, C. M.; Lautz, C.; Wurlitzer, S.; Kildae, J.; Fischer, T. M. *J. Chem. Phys.* **1997**, *106*, 1913.

5. Conclusions

In contrast to the conclusions of Feher and co-workers[10] based on thermodynamic data, we found that EA and SA were poorly miscible at all surface pressures. This conclusion is based on direct observation of phase separation using BAM and the fact that the X-ray determined molecular packing density inside the ordered domains of mixed monolayers was within 2% of the density of pure stearic acid monolayers at the same surface pressure. However, the presence of this small concentration of unsaturated chains depressed the L_2 to Ov phase transition by ~7 mN/m. This observation may shed light on the nature of the L_2 to Ov phase transition.

Acknowledgment. This work at Brookhaven National Laboratory is supported by U.S. Department of Energy, Divisions of Chemical and Materials Science, under Contract DE-AC0298CH10886 and Grant BSA/BNL LDRD and by a BNL/BSA LDRD proposal. D.K.S. and A.T.N. were supported by the National Science Foundation (Award CTS-0196119).

LA026079Y